

Applying and Assessing the Performance of Projection Method in External Mode of Princeton Ocean Model by Simulating Tidal Currents in the Persian Gulf

Ali Khosh Kholgh¹

¹ Assistant Professor, Ocean Engineering and Technology Department, Iranian National Institute for Oceanography and Atmospheric Science; a_khosh@inio.ac.ir

ARTICLE INFO

Article History:

Received: 27 May. 2023

Accepted: 12 Jul. 2023

Keywords:

Hydrodynamic
Implicit
Explicit
Numerical
Circulation

ABSTRACT

This study focused on improving the Princeton Ocean Model (POM) by proposing and implementing a new algorithm for its external mode, which solves depth-averaged two-dimensional equations of continuity and momentum transport. The goal of the new algorithm was to reduce the numerical diffusion of the model and enable the use of larger time steps for calculations. To achieve this, the Projection method was used along with the implicit discontinuity of the gravity terms in the governing equations of the two-dimensional solution of the model. The new algorithm was then evaluated for its efficiency in simulating tidal currents in the Persian Gulf. The results of the modified model were compared with those of the original model, as well as tidal fluctuations measured at several tidal stations in the Persian Gulf. The comparison showed that the modified algorithm successfully reduced the calculation time while increasing the accuracy and reducing numerical diffusion in the results.

1. Introduction

The Princeton Ocean Model (POM) developed by Blumberg and Mellor [1], is a widely used numerical model for simulating ocean dynamics in various regions of the World Ocean such as Persian Gulf([2],[3]), Red Sea ([4],[5]), China Sea ([6],[7]), Mediterranean Sea ([8], [9]) and Gulf of Mexico ([10],[11]).

<http://www.ccpo.odu.edu/POMWEB/POMRefs.htm>

and [12] gives more details of this model.

The structure of POM is modular and flexible, with separate modules for the external and internal modes. The external mode of POM is designed to solve the depth-integrated equations while its internal mode solves three-dimensional vertical structure equations. In this article, we present a new implementation of the projection method in the external mode of POM, and assess its performance in simulating tidal currents in the Persian Gulf. Our implementation builds upon the existing capabilities of POM, and leverages its modular design and flexible grid system to enable efficient and accurate simulations.

This paper is organized as follows. In section 2 method and materials used at this study including a brief description of POM, its governing equations and current and developed algorithms for solving the governing equations are presented. In section 3 an

evaluation and comparison of the performance of the original and modified version of POM model in simulation of tidal current at the Persian Gulf are presented and finally the conclusion of the study is presented in section 4.

2. Method and Materials

2.1. Numerical Model

The initial version of the POM model was presented in 1978 by Blomberg and Mellor at Princeton University, USA. Since then, the development and application of this model has been supported by various research centers, including the NOAA Geophysical Fluid Dynamics Laboratory, Princeton University, etc. This model is an open-source model and is still being changed and updated by different researchers in calculations, capabilities and speed of execution. The POM model is an efficient numerical model for simulating and predicting marine phenomena, including mixing in shallow areas, the pattern of currents and water circulation in marginal seas and open oceans, etc. More than 70 countries in the world have used this model to simulate marine phenomena, and the results of their research have been published in reputable international sources.

2.2. Governing equations

The equations that form the basis of a water circulation model express the current speed fields and the water surface elevation. Usually, two simplifying approximations of hydrostatic pressure assumption and Boussinesq approximation are used in these equations. In the first approximation, the weight of the fluid is considered equal to the water pressure, and in the second approximation, the difference in density is assumed to be negligible, except in the cases that are multiplied by the acceleration of gravity (g). These equations are written in a Cartesian coordinate system on the horizon and sigma in the vertical direction as follows:

$$\frac{\partial DU}{\partial x} + \frac{\partial DV}{\partial y} + \frac{\partial \omega}{\partial \sigma} = 0 \quad (1)$$

$$\begin{aligned} & \frac{\partial UD}{\partial t} + \frac{\partial U^2 D}{\partial x} + \frac{\partial UVD}{\partial y} + \frac{\partial U\omega}{\partial \sigma} - fVD \\ & + gD \frac{\partial \eta}{\partial x} + \frac{gD^2}{\rho_0} \int_{\sigma}^0 \left[\frac{\partial \rho'}{\partial x} - \frac{\sigma'}{D} \frac{\partial D}{\partial x} \frac{\partial \rho'}{\partial \sigma'} \right] d\sigma' \quad (2) \\ & = \frac{\partial}{\partial \sigma} \left[\frac{K_M}{D} \frac{\partial U}{\partial \sigma} \right] + F_x \end{aligned}$$

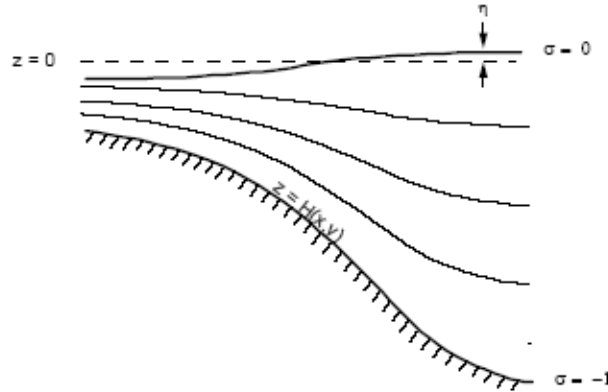


Figure 1. Specifications of the Sigma coordinate system in the vertical direction

U and V are the horizontal velocity components and ω is the vertical velocity component perpendicular to the sigma lines, which can be converted into the Cartesian velocity component from the following equation:

$$\begin{aligned} W = \omega + U \left(\sigma \frac{\partial D}{\partial x} + \frac{\partial \eta}{\partial x} \right) + V \left(\sigma \frac{\partial D}{\partial y} + \frac{\partial \eta}{\partial y} \right) \\ + \sigma \frac{\partial D}{\partial t} + \frac{\partial \eta}{\partial t} \quad (4) \end{aligned}$$

In equations 3 and 4, an average density value must be subtracted from the densities (ρ) to calculate the value (ρ'). This average value is usually the initial density

$$\begin{aligned} & \frac{\partial VD}{\partial t} + \frac{\partial UVD}{\partial x} + \frac{\partial V^2 D}{\partial y} + \frac{\partial V\omega}{\partial \sigma} + fUD \\ & + gD \frac{\partial \eta}{\partial y} + \frac{gD^2}{\rho_0} \int_{\sigma}^0 \left[\frac{\partial \rho'}{\partial y} - \frac{\sigma'}{D} \frac{\partial D}{\partial y} \frac{\partial \rho'}{\partial \sigma'} \right] d\sigma' \quad (3) \\ & = \frac{\partial}{\partial \sigma} \left[\frac{K_M}{D} \frac{\partial V}{\partial \sigma} \right] + F_y \end{aligned}$$

where x, y and z are Cartesian coordinates and the D which is representing the water depth, is calculated from the relationship $D=H+\eta$ where $H(x,y)$ is the bed topography and $\eta(x,y,t)$ is the level of the water surface. σ also represents the vertical coordinate, which changes between $\sigma=0$ at $z=\eta$ to $\sigma=-1$ at $z=-H$ (Figure 1).

field (ρ_0) which is averaged on the z levels and then transferred to the sigma coordinates like the initial density field. This procedure reduces the sequence errors caused by calculating the pressure term gradient in sigma coordinates in steep topography [13]. In these equations, the changes of the Coriolis parameter are also considered with geographic latitude. The F_x and F_y terms, which represent the horizontal diffusion terms, are obtained from the following relations:

$$F_x = \frac{\partial}{\partial x} (H\tau_{xx}) + \frac{\partial}{\partial y} (H\tau_{xy}) \quad (5)$$

$$F_y = \frac{\partial}{\partial x} (H\tau_{yx}) + \frac{\partial}{\partial y} (H\tau_{yy}) \quad (6)$$

In which:

$$\begin{aligned} \tau_{xx} &= 2A_M \frac{\partial U}{\partial x} \\ \tau_{xy} = \tau_{yx} &= A_M \left(\frac{\partial U}{\partial y} + \frac{\partial V}{\partial x} \right) \\ \tau_{yy} &= 2A_M \frac{\partial V}{\partial y} \end{aligned} \quad (7)$$

and A_M , the horizontal diffusion coefficient, is calculated in the POM model using Smagorinsky relations. The value of KM used in equations 3 and 4 are vertical diffusion coefficients, and in this model, it is possible to calculate them from different turbulence models, such as the algebraic equations of the Prandtl mixing length or the k-l and k- ϵ equations.

As can be seen, the governing equations of water circulation consist of differential equations that cannot be solved analytically for any range. Therefore, to solve them using numerical techniques, these differential equations in the desired range are converted into a series of algebraic equations and then solved using computational algorithms. In this case, the real space of the studied environment becomes a grid space, where the required unknowns are calculated on the mesh of that grid.

2.3. Algorithm for solving governing equations of POM

The equations governing the dynamics of water circulation, which were introduced in the previous section, include the fast movement of external gravity waves and the slow movement of internal gravity waves. Considering the time scale governing these two phenomena, in terms of computer calculations, it is desirable to separate these equations into depth-integrated equations called external mode and three-dimensional vertical structure equations called internal mode. This approach which is known as time-splitting and presented by ([14],[15]), forms the main structure of the algorithm for solving the three-dimensional equations governing the dynamics of water circulation in the POM model. This structure allows the free surface of water to be calculated separately from the three-dimensional calculations of velocity and thermodynamic properties.

In other words, in this algorithm, the governing equations of the external mode are extracted from the introduced governing equations by depth integration, and after applying the boundary conditions in the sigma coordinates, they are written as follows:

$$\frac{\partial \eta}{\partial t} + \frac{\partial \bar{U}D}{\partial x} + \frac{\partial \bar{V}D}{\partial y} = 0 \quad (8)$$

$$\begin{aligned} \frac{\partial UD}{\partial t} + \frac{\partial U^2 D}{\partial x} + \frac{\partial UV D}{\partial y} + \tilde{F}_x - f\bar{V}D \\ + gD \frac{\partial \eta}{\partial x} = \langle wu(0) \rangle + \langle wu(-1) \rangle + G_x \end{aligned} \quad (9)$$

$$\begin{aligned} -\frac{gD}{\rho_0} \int_{-1}^0 \int_{\sigma} \left[D \frac{\partial \rho'}{\partial x} - \frac{\partial D}{\partial x} \sigma' \frac{\partial \rho'}{\partial \sigma} \right] d\sigma' d\sigma \\ \frac{\partial \bar{V}D}{\partial t} + \frac{\partial \bar{V}^2 D}{\partial x} + \frac{\partial \bar{U}\bar{V}D}{\partial y} + \tilde{F}_y + f\bar{U}D \\ + gD \frac{\partial \eta}{\partial y} = -\langle wv(0) \rangle + \langle wv(-1) \rangle + G_y \end{aligned} \quad (10)$$

$$-\frac{gD}{\rho_0} \int_{-1}^0 \int_{\sigma} \left[D \frac{\partial \rho'}{\partial y} - \frac{\partial D}{\partial y} \sigma' \frac{\partial \rho'}{\partial \sigma} \right] d\sigma' d\sigma$$

In these equations, the bar sign on the velocities indicates their average value in the depth and from the relationships

$\bar{U} = \int_{-1}^0 U d\sigma$ and $\bar{V} = \int_{-1}^0 V d\sigma$ are determined. The wind stress components are also shown as $\langle wu(0) \rangle$ and $\langle wv(0) \rangle$ and the floor stress components are also shown as $\langle wu(-1) \rangle$ and $\langle wv(-1) \rangle$ in the above equations. In these equations, the terms G_x and G_y , which are respectively the dispersion or diffusion terms in the x and y directions, are defined as follows:

$$\begin{aligned} G_x = \frac{\partial \bar{U}^2 D}{\partial x} + \frac{\partial \bar{U}\bar{V}D}{\partial y} - \tilde{F}_x \\ - \frac{\partial \bar{U}^2 D}{\partial x} - \frac{\partial \bar{U}\bar{V}D}{\partial y} + \bar{F}_x \end{aligned} \quad (11)$$

$$\begin{aligned} G_y = \frac{\partial \bar{U}\bar{V}D}{\partial x} + \frac{\partial \bar{V}^2 D}{\partial y} - \tilde{F}_y \\ - \frac{\partial \bar{U}\bar{V}D}{\partial x} - \frac{\partial \bar{V}^2 D}{\partial y} + \bar{F}_y \end{aligned} \quad (12)$$

The parameters \tilde{F}_x and \tilde{F}_y are also defined as follows:

$$\begin{aligned} \tilde{F}_x = \frac{\partial}{\partial x} \left[H 2\bar{A}_M \frac{\partial \bar{U}}{\partial x} \right] + \\ \frac{\partial}{\partial y} \left[H\bar{A}_M \left(\frac{\partial \bar{U}}{\partial y} + \frac{\partial \bar{V}}{\partial x} \right) \right] \end{aligned} \quad (13)$$

$$\begin{aligned} \tilde{F}_y = \frac{\partial}{\partial y} \left[H 2\bar{A}_M \frac{\partial \bar{V}}{\partial y} \right] + \\ \frac{\partial}{\partial x} \left[H\bar{A}_M \left(\frac{\partial \bar{U}}{\partial y} + \frac{\partial \bar{V}}{\partial x} \right) \right] \end{aligned} \quad (14)$$

The presented relations show that if \bar{A}_M is constant in the vertical direction, the F terms in relations 11 and 12, which are used to calculate the G terms, cancel each other.

From the equations governing the external mode, it is clear that the main variables of this mode are water level fluctuations η and the averaged components of the current velocity at depth \bar{U} and \bar{V} which are based on the values calculated from the three-dimensional equations (internal mode) and are constant throughout the external mode solution period. Calculations in this mode use a small-time step that is determined based on the stability conditions and the speed of the external wave. This condition, which is specified by Courant-Friedrichs-Levy (CFL) criteria, is as follows:

$$\Delta t_E \leq \frac{1}{C_t} \left| \frac{1}{\delta x^2} + \frac{1}{\delta y^2} \right|^{-1/2} \quad (15)$$

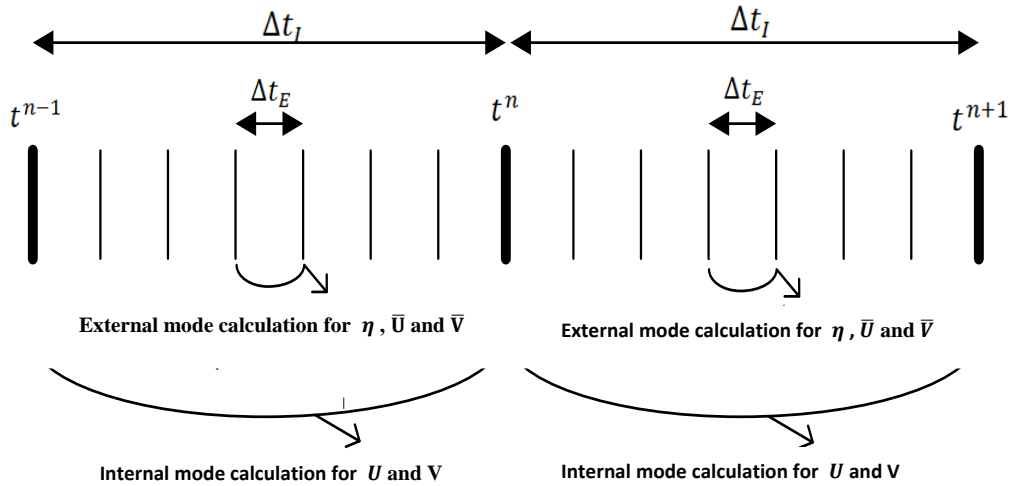


Figure 2. Relation of the internal and external mode in the POM model equation solving algorithm

The external mode solution algorithm starts by calculating the horizontal flux values in x and y directions, based on the averaged velocities in depth. Then, using the flux values calculated in the previous step and based on the continuity equation, the amount of water level fluctuations $\eta_{i,j}^{n+1}$ is determined as follows:

$$\frac{\eta_{i,j}^{n+1} - \eta_{i,j}^{n-1}}{2\Delta t_E} = (flux_{in} - flux_{out}) / Area_{i,j} \quad (16)$$

In the following, equations 9 and 10 are solved explicitly and the values of \bar{U} and \bar{V} are calculated as follows:

Where $C_t = 2(gH)^{1/2} + U_{max}$. The value of U_{max} is the expected maximum speed in the solution range. There are other restrictions, but in most problems, the CFL stability condition is determinative.

In the internal mode, considering that the effects of the rapid movement of gravity waves are removed, the CFL condition allows the use of larger time steps (Δt_I). Normally, the ratio of Δt_I to Δt_E changes in the range of 30 to 50 in coastal and ocean water circulation problems. Therefore, the model will include two calculation loops of internal mode and external mode, where the calculation loop of external mode with time step Δt_E is placed inside the calculation loop of internal mode with time step Δt_I . In this solution algorithm, all terms on the right side of equations 9 and 10 are calculated in the time steps of the internal mode and are used in all the time steps of the external mode. Figure 2 shows how to exchange information in both external and internal modes.

$$\frac{(D\bar{U})_{i,j}^{n+1} - (D\bar{U})_{i,j}^{n-1}}{2\Delta t_E} = \phi \quad (17)$$

where ϕ includes the transfer and velocity diffusion terms, water surface slope terms ($gD \frac{\partial \eta}{\partial y}$ and $gD \frac{\partial \eta}{\partial x}$), Coriolis terms and bed friction and the baroclinic pressure term. The terms related to the water level slope in these two equations are discretized as a weighted combination of new and old values of water level fluctuations as follows:

$$gD \frac{\partial \eta}{\partial x} = g \frac{D_{i+1/2,j}^n}{\Delta x} \left((1-2\alpha)(\eta_{i,j}^n - \eta_{i-1,j}^n) + \alpha(\eta_{i,j}^{n-1} - \eta_{i-1,j}^{n-1} + \eta_{i,j}^{n+1} - \eta_{i-1,j}^{n+1}) \right) \quad (18)$$

$$gD \frac{\partial \eta}{\partial y} = g \frac{D_{i,j+1/2}^n}{\Delta y} \left((1-2\alpha)(\eta_{i,j}^n - \eta_{i,j-1}^n) + \alpha(\eta_{i,j}^{n-1} - \eta_{i,j-1}^{n-1} + \eta_{i,j}^{n+1} - \eta_{i,j-1}^{n+1}) \right) \quad (19)$$

The value of $\alpha = 0$ will lead to a completely explicit solution, and as a result, the value of Δt have to be enough small to satisfy the CFL stability criteria. Therefore, in the POM model, the value of $\alpha=0.225$ has been used, and therefore, the value of Δt can be increased a little bit in the calculations.

The remaining terms of ϕ are calculated based on the values obtained from the relevant variables from the last time step of the internal mode and are considered constant during all the time steps of the external mode corresponding to that internal mode. After completing the loop calculations related to the external mode, the values of the three-dimensional velocity components in the X and Y directions are modified in such a way that their depth-averaged values are equal to the depth-averaged velocity values obtained from the external mode calculations. After this modification, by applying the continuity equation for each cell along the water column, the values of vertical velocity ω in different layers are calculated.

Further, in order to solve equations 2 and 3 and obtain the values of U and V in the new time, the calculations are divided into two explicit and implicit parts. In the explicit calculation section, the effect of horizontal diffusion terms along with bed friction, Coriolis force, and forces caused by density difference are determined on velocity changes, and in the implicit calculation

section, the effect of vertical diffusion is applied to velocity field changes. This division is due to the necessity of using small spatial steps in the vertical direction near the surface and floor for this process. In other words, if the explicit solution is used in this process, the limitation of using small time steps to satisfy the stability conditions of the solution should be observed, which will increase the calculation time.

2.4. Applying an implicit algorithm for solving two-dimensional equations in the POM

Explicitly solving the equations governing the motion of the gravitational wave in the external mode and as a result the limitation of the time step value of the calculations in wide ranges will cause the calculation time to be prolonged. Therefore, it was decided that the governing equations of this mode, which are in fact the same equations integrated in depth, using the projection method that was first introduced by Chorin [16] and using an implicit method to discretize the pressure term of the solution be made.

The use of this method, in addition to providing the possibility of using larger time steps in the external mode, also reduces the amount of numerical diffusion, which is one of the characteristics of explicit methods. In this method, as shown in Figure 3, after determining the calculation cells, the solution space is divided into horizontal and vertical blocks. The calculation variable of horizontal blocks is water level fluctuations and speed in x direction, while the calculation variable of vertical blocks is water level fluctuations and speed in y direction.

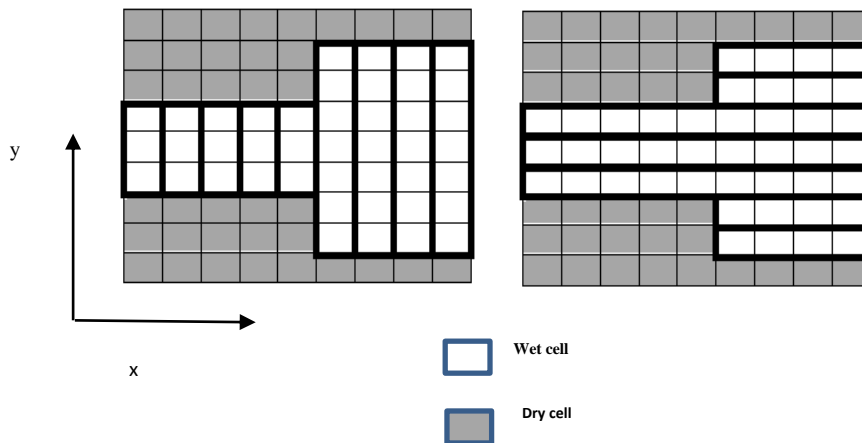


Figure 3. Schematic example of defining computational blocks in x and y direction in the implicit solution algorithm of external mode for POM

In the following, the remaining part of the momentum equations is discretizing the form of a weighted combination (β) from the implicit and explicit solution of the gravitational wave term and the explicit solution

of the other terms. Assuming $P = \bar{U}D$ and $Q = \bar{V}D$, the remaining part of the momentum equation in the x and y directions will be as follows:

$$\left(\frac{P^{n+1} - P^*}{\Delta t}\right)_{i,j} + gD_{i-1/2,j} \left(\beta \frac{\eta_{i,j}^{n+1/2} - \eta_{i-1,j}^{n+1/2}}{\Delta x} + (1-\beta) \frac{\eta_{i,j}^n - \eta_{i-1,j}^n}{\Delta x} \right) = \phi_x \quad (20)$$

$$\left(\frac{Q^{n+1} - Q^*}{\Delta t}\right)_{i,j} + gD_{i,j-1/2} \left(\beta \frac{\eta_{i,j}^{n+1/2} - \eta_{i,j-1}^{n+1/2}}{\Delta y} + (1-\beta) \frac{\eta_{i,j}^n - \eta_{i,j-1}^n}{\Delta y} \right) = \phi_y \quad (21)$$

where ϕ includes Coriolis terms, bed friction, wind stress and density changes which all are explicitly calculated and applied in the form of source-sink terms in the equation.

At the same time, the continuity equation is separated in two stages with time steps $\Delta t/2$ in such a way that in the first stage the value of η is taken from time n to $n+1/2$ and in the second stage it is brought from $n+1/2$ to $n+1$. Each of these two steps can be done in x or y direction blocks. For example, the discretized form of the continuity equation, if the equations are solved first in the x direction block and then in the y direction block, will be as follows:

$$\left(\frac{\eta^{n+1/2} - \eta^n}{\Delta t/2}\right)_{i,j} + 0.5 \left(\frac{(P_{i+1} - P_i)^{n+1} + (P_{i+1} - P_i)^n}{\Delta x} \right)_j + \left(\frac{(Q_{j+1} - Q_j)^n}{\Delta y} \right)_i = 0 \quad (22)$$

$$\left(\frac{\eta^{n+1} - \eta^{n+1/2}}{\Delta t/2}\right)_{i,j} + \left(\frac{(P_{i+1} - P_i)^n}{\Delta x} \right)_j + 0.5 \left(\frac{(Q_{j+1} - Q_j)^{n+1} + (Q_{j+1} - Q_j)^n}{\Delta y} \right)_i = 0 \quad (23)$$

As can be seen, the unknowns of equation 22 are $\eta_{i,j}^{n+1/2}$, $P_{i,j}^{n+1}$ and $P_{i+1,j}^{n+1}$ that by substituting the terms $P_{i+1,j}^{n+1}$ and $P_{i,j}^{n+1}$ from equation 20 and rewriting equation 22, an equation in terms of $\eta_{i+1,j}^{n+1/2}$,

$\eta_{i,j}^{n+1/2}$ and $\eta_{i-1,j}^{n+1/2}$ will be obtained. By applying these equations to all the cells of each x -direction block and applying the boundary conditions, a system of three-dimensional equations is obtained, by solving which the values of water level fluctuations in all the cells of each block are calculated simultaneously at the $n+1/2$ level. Next, by using equation 20, the values of current flux and speed in the x direction are also obtained at the $n+1$ time level.

After this step, the second part of the continuity equation, equation 23, is used for y -direction blocks. As can be seen, the unknowns of this relationship are $\eta_{i,j}^{n+1}$, $Q_{i,j}^{n+1}$ and $Q_{i,j+1}^{n+1}$. At this stage, by replacing the terms $Q_{i,j+1}^{n+1}$ and $Q_{i,j}^{n+1}$ from equation 21 and rewriting equation 23, an equation in terms of $\eta_{i,j+1}^{n+1}$, $\eta_{i,j}^{n+1}$ and $\eta_{i,j-1}^{n+1}$ will be obtained, which by applying these equations to all the cells of each y -direction block and applying boundary conditions, a system of three-dimensional equations is obtained, by solving which the values of water level fluctuations in all the cells of each y -direction block are calculated simultaneously at the $n+1$ level. In the following, by using the equation 21, the values of the current flux in the y -direction at the $n+1$ time scale are obtained.

Also, in order to maintain the symmetry and uniformity of the solution in one time step, first the equations are solved in the x direction and then the equations are solved in the y direction, and this order is reversed in the next time step

3. Evaluation and comparison of the performance of the original model and the modified model

In order to evaluate and compare the performance of the POM research model and the correction algorithm applied in it, the simulation of tidal currents in the Persian Gulf was put on the agenda. For this purpose, preliminary measures such as data collection including geometric and bathymetric boundaries of the solution area, tidal information in the open boundary and information of tidal fluctuations inside the solution area were carried out to validate the model results.

In Figure 4, the studied area, the location of the stations with tidal level data, as well as the bathymetry of the studied area are shown.

In this study, in order to simulate currents caused by tides in the Persian Gulf, the recorded values of water level fluctuations at Bandar Jask station shown in Figure 5, were used as open boundary conditions.

According to the scale of tidal currents, the period of adaptation of the model to the cold initial condition is several days. Therefore, by introducing the initial condition equal to the stationary state in the Persian Gulf and introducing the tidal values in Jask port as the open boundary conditions of the POM model, the

simulation of the currents caused by the tides during the months of July and August in 2018 has been done.

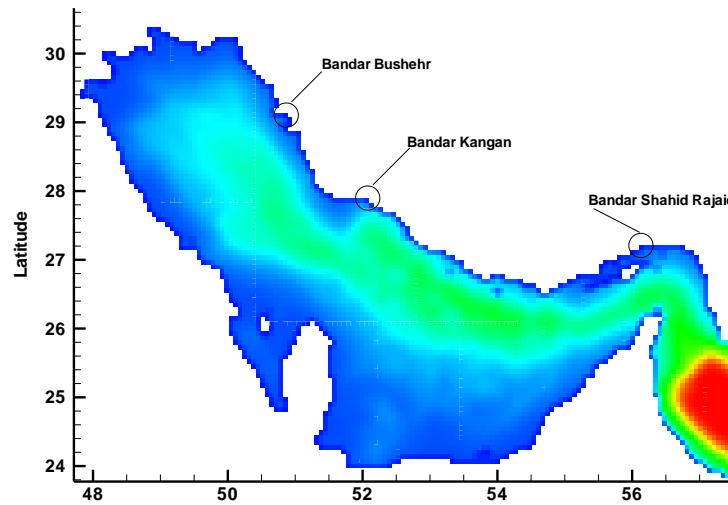


Figure 4. The studied area, its bathymetry and the location of tide measurement stations in Shahid Rajaei, Kangan and Bushehr ports

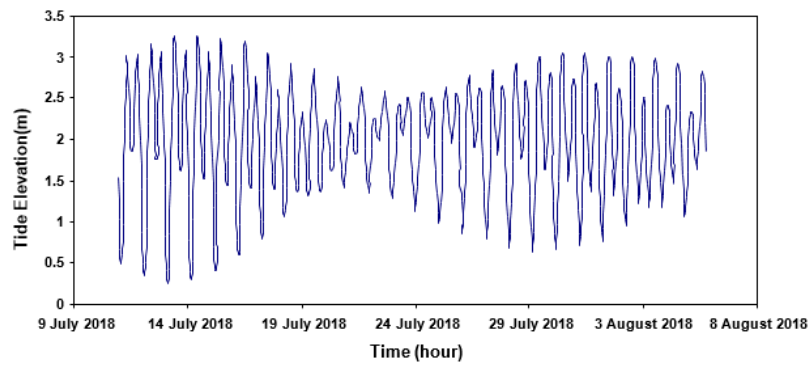


Figure 5. Tide measured at Jask station used as open boundary condition

The computational grid used in this study was in the form of square cells with dimensions of 6 km and 10 sigma layers in the vertical direction. Considering the need to satisfy the stability conditions governing the external mode of the main model, the time steps of the external and internal mode of the simulation with the original model were chosen equal to 30 and 600 seconds, respectively.

Although the implicit characteristic of the modified external mode algorithm removes the limitation of the time step of that mode, it can affect the accuracy of the results. Therefore, the external mode time step of the modified model was chosen equal to 50 seconds, and as a result, the number of external mode calculations performed within each internal mode is reduced from 20 times to 12 times. Of course, it should be noted that due to the fact that in the modified algorithm, the equations will be solved in each time step for each x and y direction blocks of computational grid, the speed

of calculations will not increase in the same proportion as the number of time steps decreases.

In order to observe and compare the results of the simulation of the tidal currents of the Persian Gulf in the mentioned time period, the recorded data of tidal fluctuations in this time period from the stations of Bandar Bushehr, Bandar Kangan and Bandar Shahid Rajai, whose locations are shown in Figure 4, has been compared with the results of the original model and the modified model at these points.

To ensure the elimination of the effects caused by unrealistic initial conditions, this comparison was made from the 10th day of the simulation, that is, from July 10 to August 10. Figures 6 show a comparison of the tidal level simulated in the mentioned stations by the original model (explicit solution of the external mode, POM-EXP) and the modified model (implicit solution of the internal mode, POM-IMP) with the data measured in these stations.

As shown in the presented graphs, the results of the modified model (POM-IMP) compared to the original model (POM-EXP) have simulated the maximum and minimum values of the water level more appropriately. This issue, which can be due to the less numerical diffusion of the modified algorithm, is more evident in Bushehr Port station, which is further away from the open boundary.

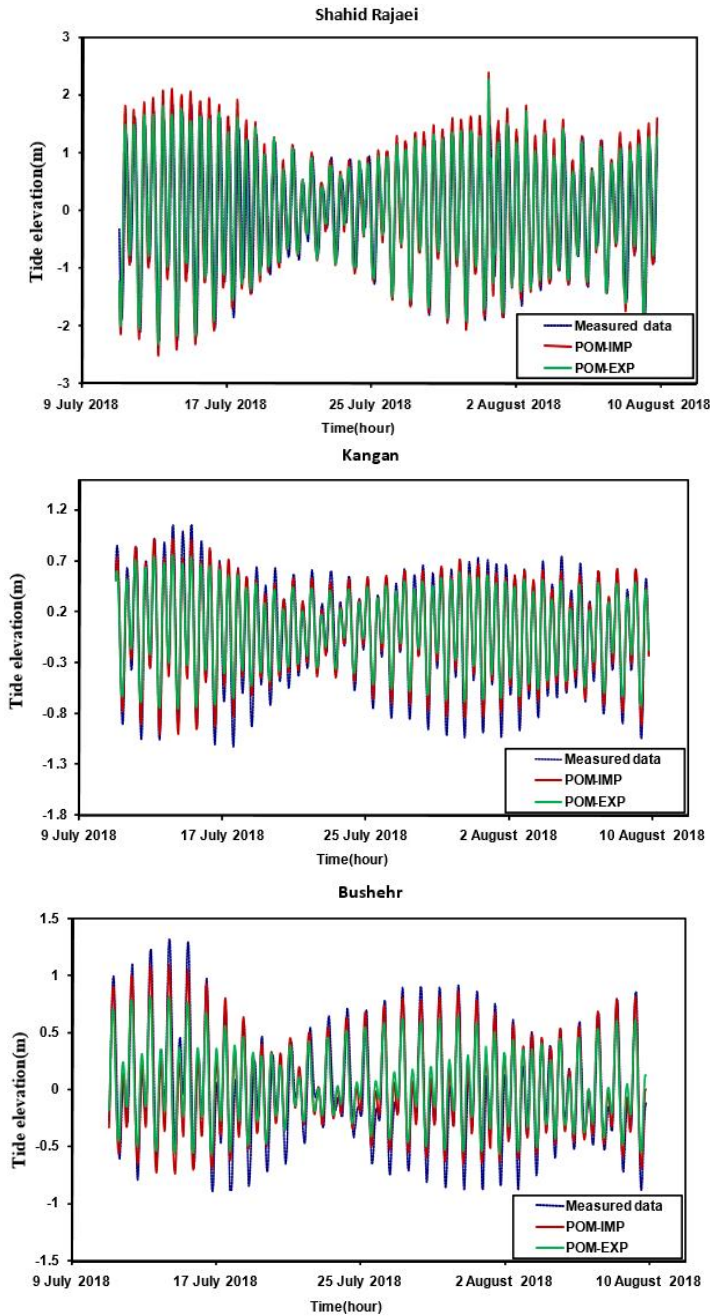


Figure 6. Comparison of water level fluctuations calculated by Original and Modified POM model with measured values in Shahid Rajaei, Kangan and Bushehr port stations

The computational time of the original model and the modified model on a personal computer for this simulation was 1853 and 1456 seconds, respectively. Therefore, in the mentioned example, with the help of the modified algorithm and a 67% increase in the time step used in the external mode, in addition to reducing

the value of numerical diffusion, the calculation speed has also increased by 21.4%.

In order to better compare the results of the two models, the Q-Q plots of the results of the two models and the measured values along with the statistical parameters of the root mean square errors (RMSE) and correlation coefficients are shown in Figure 7.

As can be deduced from these graphs, the results obtained from the implicit algorithm applied in the numerical model of POM, in the two stations of Bandar Bushehr and Bandar Kangan, have less error than the results obtained from the implementation of the original model.

5. Conclusions

Acquaintance, modification and use of research numerical models with available code is a shortcut to access a numerical model for simulating different processes.

In this article, we have presented a new implementation of the projection method in the external mode of Princeton Ocean Model (POM), and assessed its performance in simulating tidal currents in the Persian Gulf.

By comparing our results with the results obtained using the original POM model and observational data, we showed that this approach can not only simulate the dynamics of tidal currents in the Persian Gulf more accurately by reducing the numerical diffusion, but also can speed up the calculations by increasing the time step of external mode.

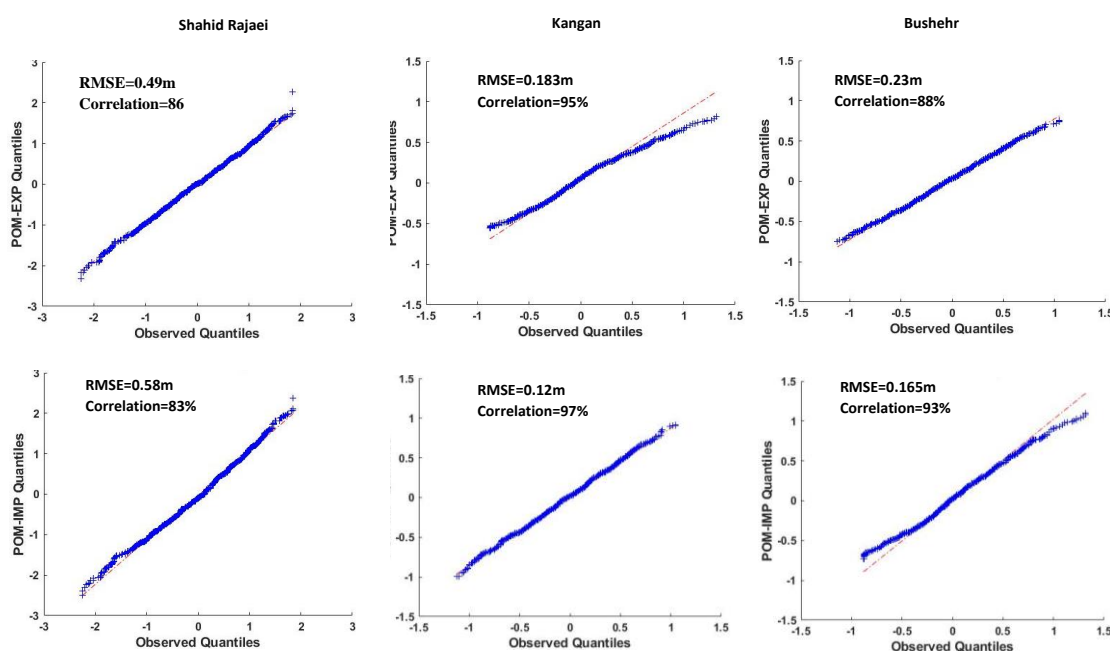


Figure 7. Q-Q Plots and statistics indexes for comparison of tidal fluctuations calculated using original model (POM-EXP, top) and the modified model (POM-IMP, bottom) with measured values in Shahid Rajaei, Kangan and Bushehr stations

8. References

- [1] Blumberg, A. F. and G. L. Mellor, 1987, A description of a three-dimensional coastal ocean circulation model. Three-Dimensional Coastal Ocean Models, edited by N. Heaps, 208 pp., American Geophysical Union.
- [2] Mosaddad, S. M., Thermocline Formation in the Persian Gulf. International Journal of Environmental Science, 5, 253-258, 2020.
- [3] Namin M. M. Bidokhti A. A. Khaniki A. K. Zadeh I. H. and Azad M. T. A Study of the Performances of Different Turbulence Schemes in Numerical Simulation of Hydrodynamics of a Semi-Closed Sea (Persian Gulf) Marine Geodesy 1-24 2016.
- [4] Clifford M. C. Horton J. Schmitz and L. H. Kantha an oceanographic nowcast/forecast system for the Red Sea J. Geophys. Res. 102(C11) 25 101-25 122 1997.
- [5] Aiki H. K. Takahashi and T. Yamagata the Red Sea outflow regulated by the Indian monsoon Cont. Shelf Res. 26(12-13) 1448-1468 2006.
- [6] Yeqiang Shu, Jinghong Wang, Huijie Xue, Rui Xin Huang, Ju Chen, Dongxiao Wang, Qiang Wang, Qiang Xie, and Weiqiang Wang, Deep-Current Intraseasonal Variability Interpreted as Topographic Rossby Waves and Deep Eddies in the Xisha Islands of the South China Sea, JPO, <https://doi.org/10.1175/JPO-D-21-0147.1>, 2022.
- [7] Liu, X. et al., A review of tidal current energy resource assessment in China, Renewable and Sustainable Energy Reviews, 145, <https://doi.org/10.1016/j.rser.2021.111012>, 2021.
- [8] Horton C. M. Clifford J. Schmitz and L. H. Kantha A real-time oceanographic nowcast/forecast system for the Mediterranean Sea J. Geophys. Res. 102(C11) 25 123-25 156 1997.

- [9] Allen J. I. P. J. Somerfield and J. Siddorn Primary and bacterial production in the Mediterranean Sea: a modeling study *J. Mar. Sys.* 33-34 473-495 2002.
- [10] Oey L.-Y. T. Ezer and H.-C. Lee Loop Current rings and related circulation in the Gulf of Mexico: A review of numerical models and future challenges in: *Circulation in the Gulf of Mexico: Observations and Models* W. Sturges and A. Lugo-Fernandez (Eds.), *Geophys. Monograph Ser.*, Vol. 161 pp. 31-56 AGU Washington DC 2005.
- [11] Ly L.N. The Gulf of Mexico Response to Hurricane Frederic Simulated with the Princeton Numerical Ocean Circulation Model Technical Report Institute for Naval Oceanography 42 pp. 1992.
- [12] Mellor, G. L., 1996, User's guide for a three-dimensional, primitive equation, numerical ocean model. Unpublished report, Atmospheric and Ocean Sciences Program, pp. 35, Princeton University, Princeton, NJ.
- [13] Mellor, G. L., T. Ezer, and L.-Y. Oey, 1994, The pressure gradient conundrum of sigma coordinate models, *J. Atmos. Ocean. Tech.*, 11, 1126-1134.
- [14] Simons, T. J., 1974, Verification of numerical models of Lake Ontario. Part I. Circulation in spring and early summer. *J. Phys. Oceanogr.*, 4, 507-523.
- [15] Madala, R. V., and S. A. Piacsek, 1977, A semi-implicit numerical model for baroclinic oceans. *J. Comput. Phys.*, 23, 167-178.
- [16] Chorin, A.J., 1968, Numerical solution of the Navier-Stokes equations, *Math. Comput.* 22, 745-762.